



Providing Choice & Value

Generic CT and MRI Contrast Agents



**FRESENIUS
KABI**

CONTACT REP

AJNR

**Neuroradiologic Applications with Routine
C-arm Flat Panel Detector CT: Evaluation of
Patient Dose Measurements**

Y. Kyriakou, G. Richter, A. Dörfler and W.A. Kalender

AJNR Am J Neuroradiol published online 7 August 2008
<http://www.ajnr.org/content/early/2008/08/07/ajnr.A1237.citation>

This information is current as
of July 28, 2025.

ORIGINAL
RESEARCHY. Kyriakou
G. Richter
A. Dörfler
W.A. KalenderNeuroradiologic Applications with Routine C-arm
Flat Panel Detector CT: Evaluation of Patient Dose
Measurements

BACKGROUND AND PURPOSE: Since the introduction of flat panel detector–equipped C-arms, the use of flat panel detector CT (FPCT) in the neuroradiologic angiography suite has become more frequent. This examination implicates its own specific radiation exposure. We used the CT dose index (CTDI) concept and adapted it to the special FPCT geometry to provide a consistent comparison with multisection head CT (cCT).

MATERIALS AND METHODS: Exposure data obtained for routine scanning during a period of 1 year were used to assess a specific dose of a total of 217 rotational scans performed in 105 patients. One hundred seventy-two scans were 3D digital subtraction angiography (DSA) scans. There were 45 scans that were performed to achieve high-quality, soft-tissue resolution. Dose measurements in cylindrical polymethylmethacrylate (PMMA) phantoms were used to determine the CTDI value and to compare it with the reference values for cCT. In addition, the dose-area product (DAP) was registered and correlated with the CTDI and corresponding dose-length product (DLP) values. Exposure data and dose values were compared with cCT.

RESULTS: Mean-weighted CTDI value of 3D-DSA was approximately 9 mGy per scan. High-quality, soft-tissue resolution FPCT scans, comparable with cCT, revealed a mean dose value of 75 mGy (reference value for cCT, $CTDI_w \sim 60$ mGy).

CONCLUSION: The high-speed scans used for 3D-DSA revealed a significantly lower $CTDI_w$ and DLP compared with clinical CT. The high-quality FPCT protocol resulted in a higher dose and should therefore be limited to acute cases, when patient transfer to a CT scanner is considered to be a disadvantage for patient management.

Flat panel detectors (FPD) mounted on dedicated gantry systems or interventional C-arms are currently used for CT scanning. These scanners are used for interventional radiology and angiography or image-guided radiation therapy units and offer large coverage of up to 200 mm.^{1–6} Volumetric imaging provided in the operating room has proved to be valuable for intraoperative procedures and is available for navigation and fusion with other preoperative or postoperative imaging modalities.^{6–8}

Neuroradiology may benefit from the dual capabilities of such scanners.^{8–12} Conventional digital subtraction angiography (DSA) can be combined with rotational digital subtraction angiography (3D-DSA). Furthermore, rotational datasets can also be used to reconstruct native or contrast CT datasets of the brain and skull. The image quality of modern C-arm scanners has improved, especially with respect to low-contrast detectability.^{4–6} The first C-arms with use of CT functionality were equipped with image intensifier tubes and had their application, especially in the very-high-contrast angiographic imaging, working with contrast differences of more than 1000 HU. Current systems are equipped with FPDs and offer a significant improvement in low-contrast resolution. Contrast differences of down to 10 HU can be detected, which is a qualitative highlight.^{1,4} Imaging of cerebral bleeding, which was

only detectable on conventional CT, now is possible within the angiography suite with use of FPCT. Nevertheless, low-contrast image quality is inferior compared with clinical CT.^{3,5,6} On the other hand, imaging of small, high-contrast targets, like intracranial microstents, seems to be superior compared with conventional multisection CT.⁹ Bone imaging with FPCT, a high-contrast target again, at least is equal to multisection CT, which is published for lumbar myelography and postmyelographic FPCT.¹⁰

The frequent use of FPCT is associated with an increase of radiation dose to the patient when FPCT is performed as an additional examination. It is not surprising that this concern has led to increased scrutiny with regard to the accuracy of radiation dose assessment to patients who undergo CT examinations. C-arm FPCT again has substantial changes in geometry, providing collimations by far higher than the 100-mm recommended integration length of the CT dose index (CTDI) standard.^{13–19} In addition, the systems use partial rotation scanning, which is expected to result in inhomogeneous dose distributions in the patient.^{6,20} It is also questionable if the common phantoms are sufficient for dosimetry with use of wide-beam fields.^{15,19} Although these scanners perform CT scanning, there is no consensus yet on estimating the patient dose for FPCT imaging. Because the systems emerged from radiography and angiography, many manufacturers provide the dose-area product (DAP) omitting any CT-specific terminology.²¹ Still, it is important for intermodality comparison reasons to adapt dose metrics used for FPCT to provide an accurate and flexible dose assessment.

In this study, we used the CTDI concepts as they are defined for standard CT and adapted them to the special C-arm

Received March 28, 2008; accepted after revision June 10.

From the Institute of Medical Physics (Y.K., W.A.K.) and Department of Neuroradiology (G.R., A.D.), University of Erlangen-Nuremberg, Erlangen, Germany.

Please address correspondence to Dr. Yiannis Kyriakou, Institute of Medical Physics, University of Erlangen-Nuremberg, Henkestr 91, 91052 Erlangen, Germany; e-mail: yiannis.kyriakou@imp.uni-erlangen.de

DOI 10.3174/ajnr.A1237

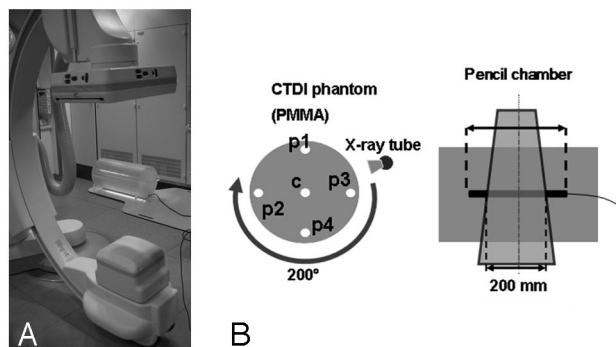


Fig 1. Measurement (A) and dosimetry setup (B) including the C-arm system and the PMMA phantom in which the ionization chamber was placed. The PMMA phantom possessed 5 bore-holes for dosimeter placement in the central and peripheral regions.

geometry to provide a consistent comparison between clinical CT and C-arm CT. The exposure data are provided for routine scanning for 1 year with use of automatic exposure control for the acquisition of 105 patients with C-arm FPCT.

Materials and Methods

Equipment

For the investigations, an Axiom Artis dBA C-arm (Siemens Medical Solutions, Forchheim, Germany) with respective acquisition and reconstruction software (DynaCT; Siemens, Forchheim, Germany) was used (Fig 1A). The system is equipped with biplane imaging components, from which only 1 is used for CT imaging. The C-arm uses a 40-cm × 30-cm FPD that allows for the reconstruction of a nontruncated volume of approximately 22 cm (in-plane) and 16 cm (in z-direction). For larger objects, truncation software is included by the manufacturer to correct for respective artifacts.² The system uses an automatic exposure control (AEC), which modulates the exposure settings (exposure time, tube current, and tube voltage) with respect to the detector entrance dose (DED).² The modulation method is attenuation based, and large differences are expected for different body regions or patient cross-sections. The user is allowed to set a respective DED to adjust the noise level. Besides this, there is no possibility for the user to interact with the AEC or the algorithm involved with the modulation. The AEC control at our system works according to a priority modulation. In a first step, the mAs level (tube current × exposure time per pulse) is changed; in a second step, with a lower priority, the tube voltage is adapted if the desired DED cannot be achieved with the mAs-modulation only.

In addition to the AEC, the system offers a DAP measurement chamber for on-line dosimetry (DIAMENTOR; PTW, Freiburg, Germany). The DAP chamber is mounted in front of the tube (behind the filter) and allows for a scan-specific measurement.

Dosimetry

We examined the exposure data of 105 patients with respect to the CTDI and its derivatives.¹³ The aim of the CTDI is to assess the integral over the dose profile along the z-direction (patient's longitudinal axis) for an infinite integration length

$$1) \quad \text{CTDI}_{\infty} = \frac{1}{C_z} \int_{-\infty}^{+\infty} dz D(z)$$

in the central and peripheral positions of a CTDI phantom, C_z being the collimated beam width as defined in Fig 2 and $D(z)$ representing

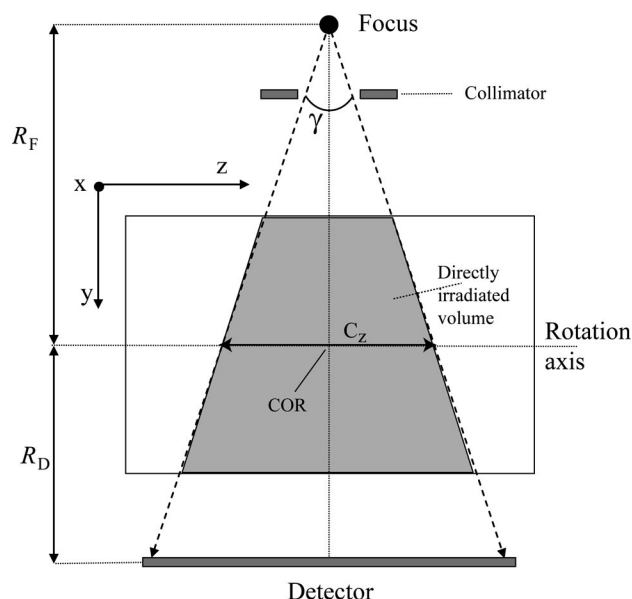


Fig 2. Geometry definitions for the y/z plane. COR is the center of rotation, C_z is the beam width at the COR (ie, collimation), and γ is the cone angle. R_F is the distance from the focal spot to the COR, and R_D is the distance from the detector to the COR.

the dose profile along the z-direction. The problem we faced is that the standard dose chambers are limited to a length of 100 mm and measure the so-called CTDI_{100} , which does not allow for an easy assessment of the integral over the complete dose profile. Following the annotations and geometry definitions of Figs 1B and 2, the maximal beam width (or collimation) C_z in the case of our C-arm CT scanner amounts to approximately 200 mm, for the center of rotation (COR) to focus distance $R_F = 785$ mm, the COR to detector distance $R_D = 415$ mm, and a detector z-extent of 300 mm, which are the standard settings for the given system.

In this case, the CTDI_{100} underestimates the ideal CTDI value, with an infinite integration range by more than 50% as shown in Boone.¹⁵ To handle this problem, we conducted the measurements with a 250-mm-long ionization chamber (iba Wellhöfer, Schwarzenbruck, Germany) to provide a better approximation of the value of CTDI, which ideally should be integrated over an infinite integration length. The values given below refer to the CTDI_{250} defined as

$$2) \quad \text{CTDI}_{250} = \frac{1}{C_z} \int_{-125 \text{ mm}}^{+125 \text{ mm}} dz D(z)$$

In the following case, we will omit the subscript 250 for simplicity. In addition, the phantom used in this study was not a typical 15-cm-long polymethylmethacrylate (PMMA) cylinder because we adapted the length to 300 mm also according to Boone.¹⁵ The diameter of the phantom was 160 mm to emulate the head region, and a 320-mm PMMA cylinder was used for the assessment of body dose according to the current CT dosimetry recommendations.^{13,16} Using peripheral and central measurements, we calculated the weighted CTDI with

$$3) \quad \text{CTDI}_w = \frac{1}{3} \text{CTDI}_c + \frac{2}{3} \text{CTDI}_p$$

where CTDI_c is measured in the central hole, and CTDI_p is the mean value over 4 peripheral measurements for a half-scan acquisition (Fig 1B). The CTDI values were normalized to 100 mAs.

The dose-length product (DLP) for the acquisitions was calculated with $DLP = CTDI_w \times C_z$ because 1 rotation covers the complete head. The values of $CTDI_w$ and DLP were scaled by the mAs-values Q_i , set by the AEC for each examination i to give the patient-specific value and $CTDI_i = (Q_i/100 \text{ mAs}) \times CTDI$ and $DLP_i = (Q_i/100 \text{ mAs}) \times DLP$ for patient i respectively. The value of the DAP was measured on-line by the system. It was examined with respect to its correlation to the CTDI measured in the phantom.

Measurement Protocols

For neuroradiologic applications, 2 protocols were used as set up by the manufacturer. A fast acquisition protocol with a single rotation time of 5 seconds was used for acquisition of 3D-DSA. This high-speed protocol acquires 2 subsequent series with 133 projections each over an angular rotation range of 200°. The high-speed protocol starts with a native mask acquisition run for subsequent subtraction, which is followed by a contrast-filled run. Contrast agent application (Iomeron 300; Bracco Altana Pharma, Germany) was done automatically with use of an appropriate injector (ProVis Mark V; Medrad, Warrendale, Pa), the contrast flow rate was in the range of 1.5 to 2.5 mL s⁻¹, and injection time was 7 seconds (delay 2 s).

A high-quality acquisition protocol uses a 200° run for 20 seconds for the acquisition of 496 projections. The high-quality protocol was performed without contrast injection usually. The DED setting was routinely set to a value of 0.36 $\mu\text{Gy/projection}$ for the high-speed protocol and 1.2 $\mu\text{Gy/projection}$ for the high-quality protocol.

Patient Cases

A total of 217 rotational head scans were performed in 105 patients. The high-speed protocol was used with intra-arterial contrast injection for 172 of 217 rotational scans, which were 3D-DSA scans, respectively. Most of the 3D-DSA examinations (72 patients) were used to assess intracranial aneurysms, less frequent were the cases of patients with intracerebral arteriovenous malformations, arteriovenous fistula, intracranial stenoses, or acute cerebral artery occlusions, respectively.

There were 45 of the 217 scans that were performed with a high-quality acquisition protocol to achieve soft tissue (low-contrast) resolution datasets. All high-quality scans were carried out without additional contrast agent injection. The high-quality scans were performed in patients who experienced intracranial hemorrhage to exclude secondary bleeding; in most cases, patients had primarily ruptured intracranial aneurysms.¹¹ Additional indications for high-quality scans were assessment of external ventricular drainage or exclusion of a primarily unnoticed bleeding during an intracranial intervention such as an arteriovenous malformation or vessel recanalization in patients with stroke.

All scans were uncollimated (full-field) head scans, in which some of the patients were scanned twice for preoperative and postoperative controls or in 3D-DSA when necessary. No special requirements were needed for this study because we collected the exposure data retrospectively.

In addition to the head scans, we included 7 exemplary spinal intervention scans (eg, myelography) to take body scans into account as well, though the use of C-arm CT for body scans is currently very limited.

Evaluation

The CTDI and the DLP were determined for voltages 70, 81, 90, 102, 109, and 125 kV, which are available to be set manually at the scanner.

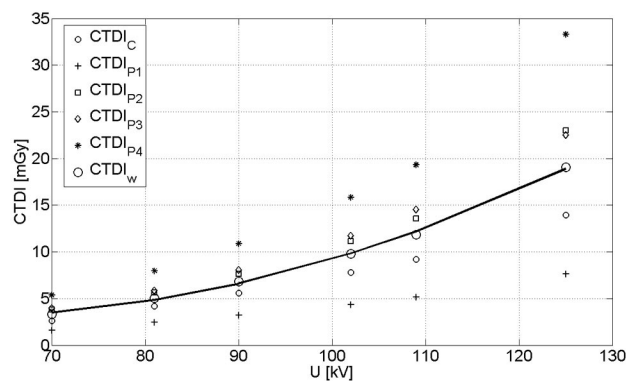


Fig 3. CTDI values for center, periphery, and the calculated $CTDI_w$. The solid line represents a quadratic fit for the $CTDI_w$ which was used for subsequent calculations. The correlation coefficient amounted to $R = 0.98$.

We applied a polynomial fit for the CTDI as a function of voltage to consider tube voltage values, which were set by the AEC and were not directly measured in the phantom. This approximation is well suited because a smooth function is expected.³

Patients were sorted according to the type of scan and the body region investigated. This arrangement resulted in 172 scans by use of the high-speed protocol and 45 scans by use of the high-quality protocols for head/brain studies. The CTDI and DLP values were calculated for each patient, and a histogram of both values with respect to all patient scans was generated.

Results

Assessment of the CTDI

The CTDI measured as a function of tube voltage, which is shown in Fig 3 (normalized to 100 mAs). In addition, the plot shows the CTDI values for the center ($CTDI_C$) and the 4 peripheral positions ($CTDI_{P1}$, $CTDI_{P2}$, $CTDI_{P3}$, and $CTDI_{P4}$). The separate CTDI values demonstrate the inhomogeneity of the dose distribution for the half-scan acquisition. Similar CTDI values are expected only for the positions p2 and p3, which are geometrically symmetric with respect to the trajectory of the tube. Position p4 results in the highest dose value because the tube traveled below the table in this specific case. The contrary holds for position p1; the difference in the CTDI compared with the lower position p2 amounted to a factor of 3.1 on average.

The typical voltage for head/brain examination ranges between 70 kV and 80 kV which is in good agreement with the measured data and corresponds to $CTDI_w$ values between 3.7 and 5.2 mGy normalized to 100 mAs, respectively. The corresponding $CTDI_w$ value for a typical 80-kV CT scan with a clinical scanner amounts to 4.0 to 6.0 mGy.³ A quadratic fit approximates the dependence between $CTDI_w$ and tube voltage very well (correlation coefficient $R = 0.98$), in which the $CTDI_w$ reflects both the tube voltage and the mAs value of the examination. As mentioned previously, this step is necessary because the AEC controls both voltage and mAs values.

For the 320-mm PMMA cylinder (body phantom), only the values for 125 kV were measured because the AEC system adjusted the tube voltage for the patient spine scans to values of more than 122 kV. With the current protocol, a CTDI value

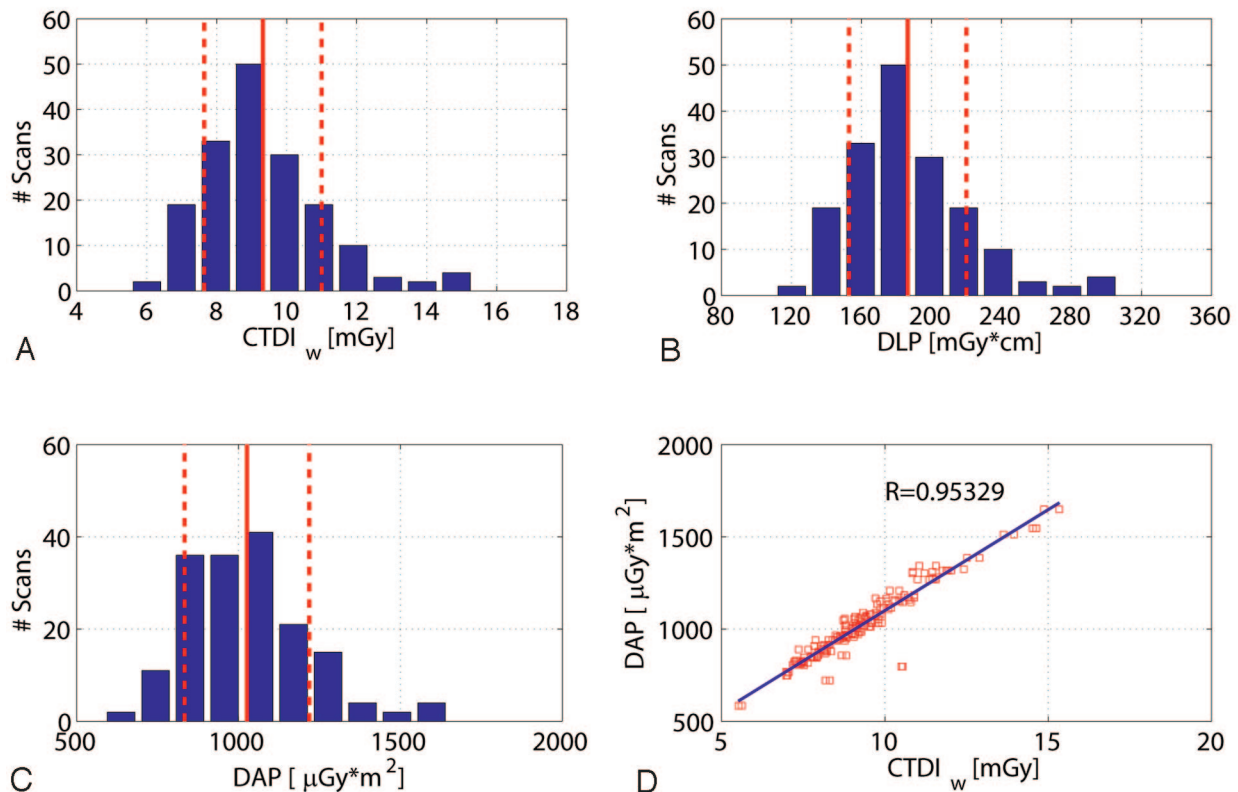


Fig 4. Dose values for 172 patient scans regarding the high-speed (HS) protocol. *A*, *B*, and *C* show the histogram of the number of patient scans regarding the CTDI_w, DLP, and DAP. The distributions are similar for the 3 dose measurement techniques. The DAP measured on-line shows a good linear correlation to the estimated CTDI_w value (*D*). Note: The red lines and red dotted lines indicate the mean value and SD.

of 8.6 mGy (normalized to 100 mAs) was measured for the body phantom. The value is comparable with CTDI measurements for clinical CT and is in agreement with exemplary values reported in Kalender's *Computed Tomography*³, which vary between 6 and 8 mGy for a 320-mm cylindrical PMMA phantom at 120 kV.

Scan-Specific Dose Values

The mean voltage for the high-speed scan with 0.36 $\mu\text{Gy}/\text{pulse}$ detector entrance dose was held constant at 70 kV. Only the mAs value was modulated with each patient with use of a mean value of 259 ± 46 mAs (mean \pm SD). The high-dose/high-image quality protocol resulted in a mean tube voltage of 79 ± 3.2 kV and used a mean value of 1592 ± 54 mAs per rotation (ie, per scan). As expected, the exposure setting remained fairly constant because the interpatient differences in attenuation are small for head examinations.

Figure 4 shows a histogram of the CTDI_w, DLP, and DAP values for all scans regarding the high-speed protocol. As already mentioned, the DAP values were measured on-line by the scanner. The CTDI_w values were 9.3 ± 1.6 mGy (mean \pm SD), and the DLP amounted to 186.6 ± 33.1 mGy \times cm. The measured DAP was distributed approximately $1026 \mu\text{Gy} \times \text{m}^2$, with an SD of $192 \mu\text{Gy} \times \text{m}^2$ calculated for the 172 scans. The SD of the values showed a relatively low interpatient variation as expected ($<20\%$). The correlation of the measured DAP and the estimated CTDI_w was very good ($R = 0.953$) as shown in Fig 4D.

Similar to the results shown in Fig 4, Fig 5 presents the

CTDI_w, DLP, and DAP values for the high-dose/high-quality scan. The CTDI_w value was 75.1 ± 5.2 mGy, and the DLP amounted to 1506.1 ± 112.7 mGy \times cm. The measured DAP resulted in $7377.4 \pm 291.9 \mu\text{Gy} \times \text{m}^2$ per rotation. Again the correlation between the CTDI_w and the DAP is very good ($R = 0.953$).

For the 7 spine scans, the average CTDI_w amounted to 85.1 ± 1.1 mGy per scan over all spine scans at tube voltage settings varying between 122 and 125 kV.

Protocol Comparison

The dose assessment revealed a dose discrepancy between the high-speed and high-quality protocols by a factor 6.0 to 8.0 on average. However, only 45 scans of 217 were performed in the high-dose mode, and the higher-dose levels were only used selectively when special indications were given as mentioned in the Patient Cases section. The spectrum of special indications for high-quality protocols included, for example, patients with subarachnoid hemorrhage, when rebleeding before or after an aneurysm-coiling procedure had to be ruled out. The high-quality protocol was used to assess intracerebral hemorrhage (eg, in patients who underwent intra-arterial thrombolysis) as well. Recapitulatory, the assessment of low-contrast difference targets like blood was seen as an indication for the high-quality protocol.

Figure 6 shows respective images resulting from a high-speed and a high-quality scan for the same patient and section, in which the high-quality protocol shows superior image quality. As expected from the dosimetric results, the noise in the

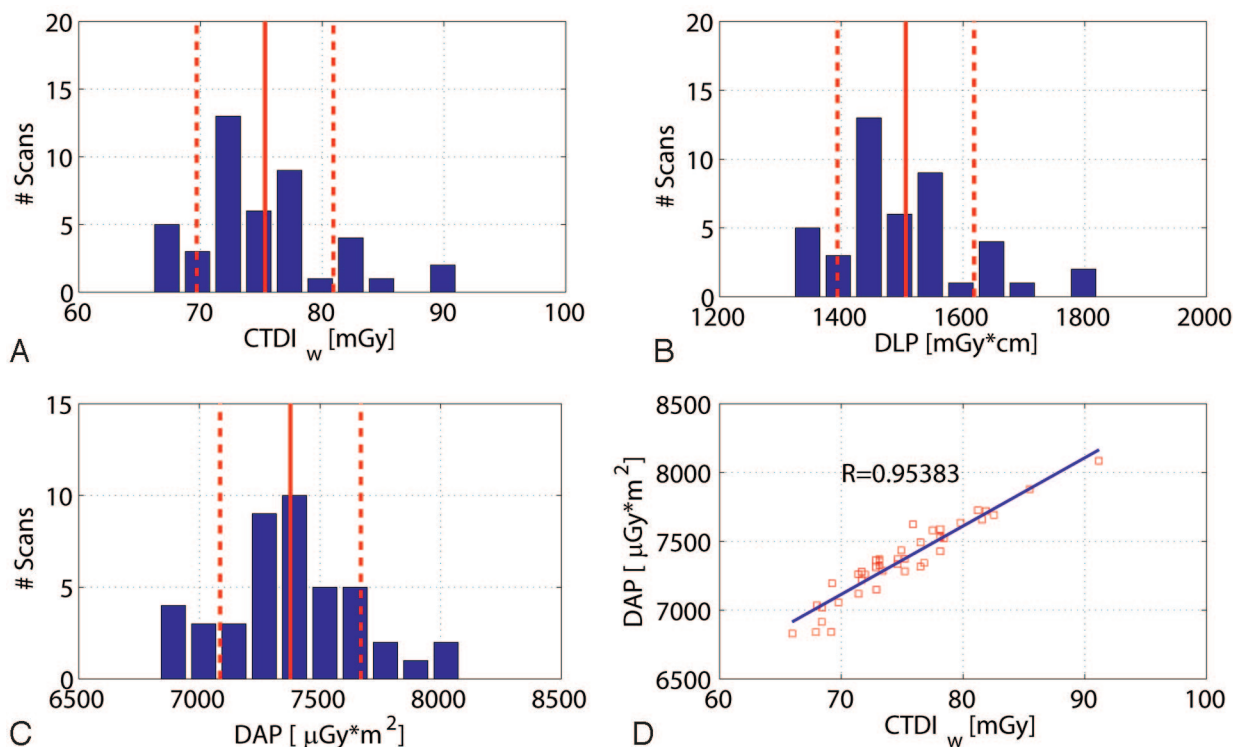


Fig 5. Dose values for 45 patient scans with use of the high-quality protocol. *A*, *B*, and *C* show the histogram of patient scans with respect to the CTDI, DLP, and DAP. The distributions are similar for the 3 dose measurement techniques. The DAP measured on-line shows a good linear correlation to the estimated CTDI_w value (*D*). Note: The red lines and red dotted lines indicate the mean value and SD.

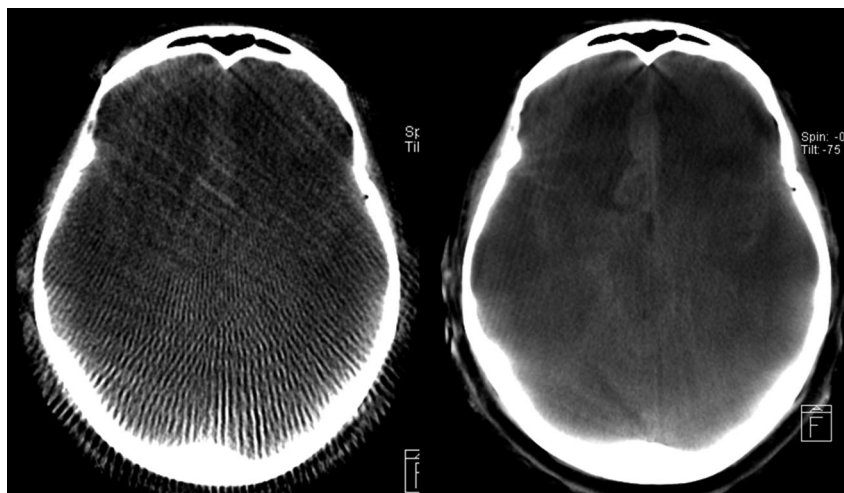


Fig 6. Qualitative comparison of an HS reconstruction (*left side*) and HQ (*right side*) for the same patient and section with respect to diagnostic image quality. Because of the superior image quality, the subarachnoid bleeding can be clearly diagnosed on the HQ image. The HS image seems to be only adequate for a rough anatomic orientation.

high-quality image seems to be much lower compared with the high-speed scan. The sampling artifacts originating from the small number of projections in high speed are quite distinct, and in high-speed protocols low tissue resolution is nearly nonexistent. Hence, in the high-speed protocol, typically it is not possible to detect intracranial hemorrhage.

Discussion

FPCT is increasingly used in the angiography suite; therefore, patient dose concerns come to the forefront. Because the method is relatively new, the adaptation of interventional radiology to CT with respect to dose considerations is not final-

ized. C-arm CT provides enhanced, 3D anatomic information that may result in, for example, better guidance and navigation during interventional procedures. Even low-contrast intracranial hemorrhage can be diagnosed, though contrast resolution seems to be inferior compared with cCT (Fig 7).

In this study, we combined technical dose measurements with a respective assessment of the exposure data during daily routine without changing the medical workflow. State-of-the-art systems were used along with the current standards in CT dosimetry. The CT dosimetry measures were correlated to the standard radiographic dose metric DAP, which is currently measured on-line for each investigation on fluoroscopic or

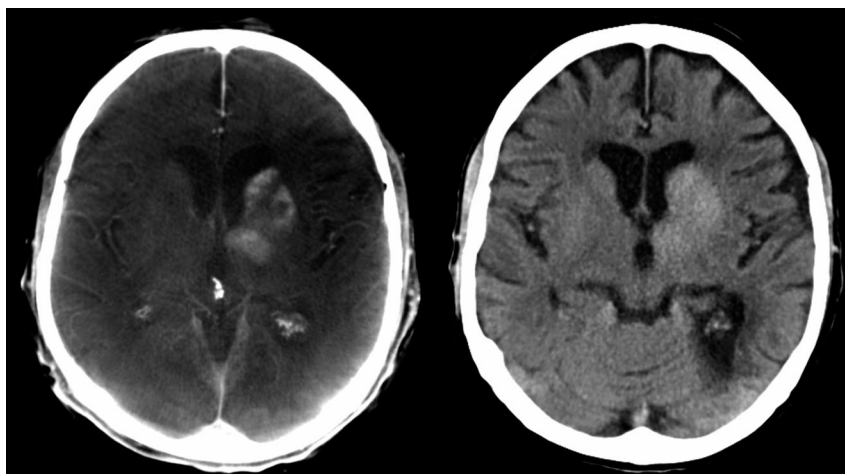


Fig 7. Mechanical thrombolysis of a carotid-T-occlusion. The reperfusion resulted in enhancement of contrast agent in the basal ganglia, which was injected during mechanical recanalization. High-quality scan (*left side*) was performed to exclude hemorrhage. This finding was confirmed on follow-up cCT, which was performed the next day (*right side*).

radiographic systems. The combination of on-line DAP measurement and CTDI calibration seems to provide appropriate means for comparing modalities and providing on-line estimates of patient dose during intervention. A combination with respective conversion factors would, in addition, provide real-time estimates of effective dose^{18,20} according to the standards currently used for conventional CT. Other authors such as Schueler et al²¹ also investigated the radiation dose with respect to 3D rotational cerebral angiography (3DRA) and recorded mainly the skin dose and the cumulative incident dose for 3DRA scans (eg, 33 mGy for their standard 3DRA acquisition mode) by using the DAP to compare with bi-planar DSA. Although it is possible to calculate the cumulative incident dose values for our scans (eg, 38.1 mGy for the standard high-speed scans at the interventional reference point²¹), we cannot use the data for a detailed comparison because several geometric parameters (field size, bow-tie filter etc) as well as the exposure data are different and some are not available in Schueler et al.²¹ We agree with the authors that for 3DRA or, in general, 3D acquisitions with C-arms, the x-ray field area can extend beyond the edges of the skull. As a result, the total DAP for a complete 3D acquisition could overestimate the patient area exposed and thus overestimate the stochastic risk, which seems to be the reason for some outliers in Figs 4D and 5D. Nevertheless, we showed here, with respect to the connection of both fluoroscopic and CT imaging, high correlation between the CTDI and the DAP; an efficient calibration method as well as calculation of correction factors with respect to error sources²¹ will be part of future work.

A minor drawback of this study may be the use of the CTDI; this holds both for the case of conventional cCT and FPCT dosimetry, as the efficiency of the index itself is currently under discussion.¹³⁻¹⁹ Although the current CTDI standard can be used as a consistent comparison measure for the validation, it is not considered as a tool for accurate patient dosimetry. For example, use of Monte Carlo tools (ImpactMC; VAMP, Erlangen, Germany) for the simulation of dose allows demonstrating the inhomogeneity of the dose distribution for partial scans of 200° for both head and pelvis scans (Fig 8A and B). Thus, in addition to the CTDI concepts, which are based on simple cylindrical phantoms, 3D dose dis-

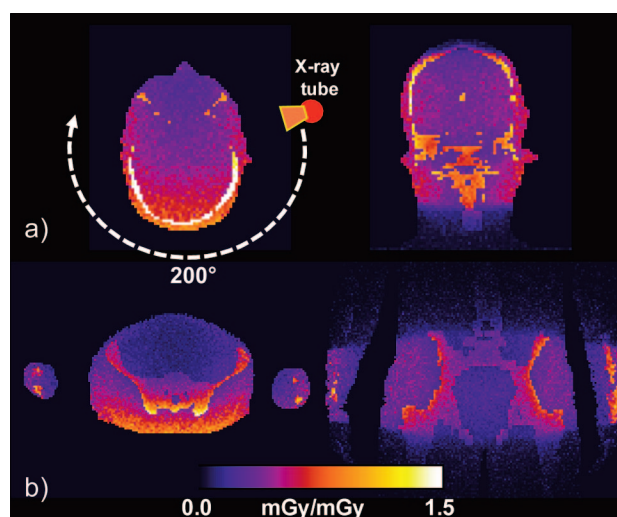


Fig 8. Example of 3D dose distributions calculated by Monte Carlo simulations for 2 phantom planes (axial and coronal) with use of an anthropomorphic phantom for a 200° C-arm FPCT scan in relative units representing head and pelvis scans. The axial section nicely demonstrates the inhomogeneity of the dose distribution for a partial scan.

tributions obtained either by simulation or by measurement can provide a more accurate look at the patient-specific distribution of dose (eg, for noncylindrical and anthropomorphic phantoms). In the latter case, 3D dose distributions can be used to estimate further parameters such as organ dose and effective dose, which are more appropriate for the quantification of patient dose.

The evaluation shows that the herein used routine measurement protocols are quite different with respect to dose and image quality. Dose varied over a factor of 6.0 to 8.0 on average between 2 specialized protocols. As the expected noise level will be a factor $\sqrt{6.0}$ to $\sqrt{8.0}$ smaller, it can be expected that the high-dose protocol will provide the overall better image quality, both for intervention and sometimes to even fulfill diagnostic-CT criteria.^{2,6,12} The high-speed mode shows a CTDI_w of approximately 9 mGy ($\text{DLP} \approx 180 \text{ mGy} \times \text{cm}$), whereas the high-quality resulted in a mean $\text{CTDI}_w \approx 75 \text{ mGy}$ ($\text{DLP} \approx 1500 \text{ mGy} \times \text{cm}$). For comparison, we extracted the reference dose values for clinical CT from the German Federal

Office for Radiation Protection (BfS) report.²² For head CT, the reference CTDI_w for routine investigations amounts to 60 mGy, whereas the DLP is given with 1050 mGy × cm. For the investigated cases on the C-arm scanner, a full-field acquisition was assumed (which is routinely used), whereas the reference values for DLP were gathered according to the specific protocols of the users, which may amount to scan lengths clearly below 20 cm for head scans. Typical CT acquisition lengths for the head can vary depending on the medical indication. The recommendations of the BfS are based on long-term studies monitoring the routine CT use for the specific application.²²

The high-speed scan, which is the most common among the C-arm CT applications, resulted in a clearly lower CTDI_w and DLP compared with clinical CT. The high-quality C-arm protocol resulted in a higher dose and should therefore be limited to special and acute cases when very good image quality comparable with standard head CT is needed.

The use of C-arm CT can be compared with standard CT in exposure and can vary from very low to high dose depending on the protocols used and cannot be ignored. Of course, this dose application has to be regarded with respect to the total exposure during intervention in which additional fluoroscopy or DSA scans (2D) are often necessary. C-arm CT combined with suitable software (eg, navigation) may support the clinical workflow and can result in a lower dose by simply reducing the overall exposure time.⁶ In addition, CT-guided interventions have the potential to minimize the additional fluoroscopic time in the operating room needed for control scans and, perhaps, also additional postoperative CT scans. Additional developments regarding the improvement of image quality for these systems will potentially result in a dose reduction for the same image quality.²⁻⁶ The use of thin-collimated scans or advanced methods such as multi-resolution local tomography could also help to maintain image quality in a volume of interest while reducing patient dose.^{3,6} Furthermore, more sophisticated AEC methods as well as spectral optimization (eg, tube filtration) combined with improved reconstruction algorithms could lead to additional improvements.⁶

Nevertheless, the applied dose is an important issue and has to be further investigated compared with standard CT and certainly as compared with the complete interventional procedure circle, including fluoroscopy and DSA. Also of interest and the subject of additional investigations is the exposure of medical personnel from CT in the angiography suite. Common dose metrics or calibration methods combining CT-like metrics such as the CTDI and radiography metrics such as the DAP would be helpful with respect to a comparison of modalities and applications. In addition, more studies should not

only look at the dose but also carefully evaluate the achieved image quality and the impact of specific dose reduction steps.

Conclusion

The high-speed scans used for 3D-DSA revealed a significantly lower CTDI_w and DLP compared with clinical CT. The high-quality FPCT protocol resulted in a higher dose and should therefore be limited to acute cases, when patient transfer to CT scanner is considered to be of disadvantage for patient management.

References

1. Groh BA, Siewerdsen JH, Drake DG, et al. **A performance comparison of flat-panel imager-based MV and kV cone-beam CT.** *Med Phys* 2002;29:967–75
2. Zellerhof M, Scholz B, Röhrnschopf E, et al. **Low contrast 3D-reconstruction from C-arm data.** *Progress Biom. Opt Imag Proc SPIE* 2005;5745 (1):646–55
3. Kalender WA. *Computed Tomography*. 2nd ed. New York: Wiley-VCH; 2005
4. Daly MJ, Siewerdsen JH, Moseley D, et al. **Intraoperative cone-beam CT for guidance of head and neck surgery: assessment of dose and image quality using a C-arm prototype.** *Med Phys* 2006;33:3767–80
5. Fahrig R, Dixon RL, Payne T, et al. **Dose and image quality for a cone-beam C-arm CT system.** *Med Phys* 2006;33:4541–50
6. Kalender WA, Kyriakou Y. **Flat-detector CT (FD-CT).** *Eur Radiol* 2007;18:828–37
7. Jaffray DA, Siewerdsen JH, Wong J, et al. **Flat-panel cone-beam computed tomography for image-guided radiation therapy.** *Int J Radiat Oncol Biol Phys* 2002;53:1337–49
8. Heran NS, Song JK, Namba K, et al. **The utility of DynaCT in neuroendovascular procedures.** *AJNR Am J Neuroradiol* 2006;27:330–32
9. Richter G, Engelhorn T, Struffert T, et al. **Flat panel detector angiographic CT for stent-assisted coil embolization of broad-based cerebral aneurysms.** *AJNR Am J Neuroradiol* 2007;10:1902–08
10. Engelhorn T, Rennert J, Richter G, et al. **Myelography using flat panel volumetric computed tomography: a comparative study in patients with lumbar spinal stenosis.** *Spine* 2007;15:32:E523–27
11. Doerfler A, Wanke I, Egelhof T, et al. **Aneurysmal rupture during embolization with Guglielmi detachable coils: causes, management, and outcome.** *AJNR Am J Neuroradiol* 2001;22:1825–32
12. Doelken M, Struffert T, Richter G, et al. **Flat-panel detector volumetric CT for visualization of subarachnoid hemorrhage and ventricles: preliminary results compared to conventional CT.** *Neuroradiology* 2008;50:517–23
13. Shope T, Gagne R, Johnson G. **A method for describing the doses delivered by transmission x-ray computed tomography.** *Med Phys* 1981;8:488–95
14. Dixon RL, Munley ML, Bayram E. **An improved analytical model for CT dose simulation with a new look at the theory of CT dose.** *Med Phys* 2005;32:3712–28
15. Boone JM. **The trouble with CTDI100.** *Med Phys* 2007;34:1364–72
16. Leitz W, Axelson B, Szendro G. **Computed tomography dose assessment- a practical approach.** *Rad Prot Dosimetry* 1995;57:377–80
17. Nakonechny KD, Fallone BG, Rathee S. **Novel methods of measuring single scan dose profiles and cumulative dose in CT.** *Med Phys* 2005;32:98–109
18. McCollough CH, Schueler BA. **Calculation of effective dose.** *Med Phys* 2000;27:828–37
19. Mori S, Endo M, Nishizawa K, et al. **Enlarged longitudinal dose profiles in cone-beam CT and the need for modified dosimetry.** *Med Phys* 2005;32:1061–69
20. Deak P, Van Straten M, Schrimpton P, et al. **Validation of Monte Carlo tool for patient-specific dose simulations in multi-slice computed tomography.** *Eur Radiol* 2008;18:759–72
21. Schueler BA, Kallmes DF, Cloft HJ. **3D Cerebral angiography: radiation dose comparison with digital subtraction angiography.** *AJNR Am J Neuroradiol* 2005;26:1898–901
22. **Bundesamt für Strahlenschutz, Diagnostische Referenzwerte für radiologische Untersuchungen.** *Bundesanzeiger* 2003;143:17503–10